NANO LETTERS

Letter

pubs.acs.org/NanoLett

# Acoustic Phonon Lifetimes and Thermal Transport in Free-Standing and Strained Graphene

Nicola Bonini,*[,†] Jivtesh Garg,[‡] and Nicola Marzari[§]

[†]Department of Physics, King's College London, London WC2R 2LS, United Kingdom

[‡]Department of Mechanical Engineering, Massachusetts Institute of Technology, Cambridge, Massachusetts 02139, United States

[§]Theory and Simulation of Materials, École Polytechnique Fédérale de Lausanne, 1015 Lausanne, Switzerland

Supporting Information

**ABSTRACT:** We use first-principles methods based on density functional perturbation theory to characterize the lifetimes of the acoustic phonon modes and their consequences on the thermal transport properties of graphene. We show that using a standard perturbative approach, the transverse and longitudinal acoustic phonons in free-standing graphene display finite lifetimes in the long-wavelength limit, making them ill-defined as elementary excitations in samples of dimensions larger than ∼1 μm. This behavior is entirely due to the presence of the quadratic dispersions for the out-of-plane phonon (ZA) flexural modes that appear in free-standing low-dimensional systems. Mechanical strain lifts this anomaly, and all phonons remain well-defined at any wavelength. Thermal transport is dominated by ZA modes, and the thermal conductivity is predicted to diverge with system size for any amount of strain. These findings highlight strain and sample size as key parameters in characterizing or engineering heat transport in graphene.

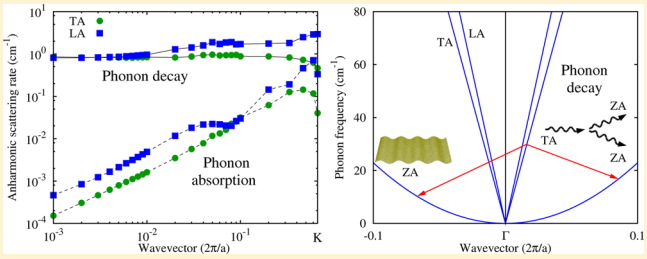


**KEYWORDS:** *Graphene, thermal transport, strain, anharmonicity, phonon lifetime, first-principles calculations*

After the first experimental measurement of its thermal conductivity—that reported values between 2000 and 5000 W/(mK) at room temperature,[1,2] the highest of any material—graphene has been hailed for its extraordinary thermal transport properties and its possible applications to heat management in nanoscale devices. Many research efforts have since been devoted to understanding graphene's thermal conductivity, but the overall scenario remains complex or even controversial (see ref 3 and citations therein).

On the experimental side, several groups reported quite different results for the thermal transport properties of suspended graphene. Faugeras et al.,[4] studying large graphene membranes prepared via micromechanical cleavage techniques, argued that the thermal conductivity of this system may actually be not as high as initially reported: the value measured is around 600 W/(mK) at 660K, still quite high but from 5 to 8 times lower than initial room temperature estimates. Ruoff's group[5,6] investigated thermal transport in suspended and supported graphene grown by chemical vapor deposition on Cu and reported a room temperature conductivity ranging from (2500 + 1100/ −1050) to (2600 ± 900 to 3100 ± 1000) W/(mK) for suspended graphene that decreases to (370 + 650/−320) W/(mK) for supported graphene—the latter is comparable to the thermal conductivity range of 479−680 W/(mK) recently measured for exfoliated graphene on a silicon dioxide support.[7] Recently, Lee et al.[8] reported values for the conductivity ranging from ∼1800 W/(mK) near room temperature to ∼700 W/(mK) at 500 K for mechanically exfoliated graphene.

From the theoretical point of view the thermal conductivity in low-dimensional systems has been subject of great debate for many years. Numerical simulations for 2D and 1D model systems indicate that thermal conductivity depends on the size of the sample—a logarithmic (power law) divergence with system size for 2D (1D) systems.[9] However, these models do not include out-of-plane (for 2D systems) or out-of-line (for 1D systems) degrees of freedom, and their ability to provide a proper description of realistic systems remains unclear. For instance, it is interesting to note that recent molecular dynamics (MD) simulations on carbon nanotubes[10] (quasi 1D systems) have shown that the thermal conductivity of these systems converges with system size.

In the case of graphene, Klemens pointed out that the thermal conductivity above room temperature should show a logarithmic divergence with system size.[11] This conclusion is based on a model[12] that considers only the two in-plane acoustic branches [longitudinal (LA) and transverse (TA) modes] and their intrinsic relaxation rates due to anharmonic three-phonon Umklapp processes. The model, however, approximates the anharmonic coupling terms with an average

**Received:** August 3, 2011
**Revised:** May 11, 2012
**Published:** May 16, 2012

   dx.doi.org/10.1021/nl202694m | *Nano Lett.* 2012, 12, 2673−2678

Grüneisen parameter and neglects the contribution of the out-of-plane phonon modes (ZA)—the so-called bending or flexural modes—that, because of their quadratic-like dispersion, have a very low group velocity. To what extent and in which temperature range these out-of-plane modes can be disregarded is unclear. Indeed, in graphene and, more in general, in layered crystals, these vibrations are known to determine not only the negative thermal expansion coefficient[13] but also the low-temperature behavior of both the specific heat and the thermal conductance.[14] Quite interestingly, recent studies[7,15] indicate that these modes could actually play a key role in the thermal transport properties of graphene even above room temperature. These conclusions are based on a numerical solution of the phonon Boltzmann transport equation where phonon modes and three-phonon coupling terms are obtained from an empirical interatomic potential.

The main purpose of this paper is to provide a first-principles characterization of the phonon−phonon scattering rates of the acoustic modes of graphene, in order to elucidate their role in thermal transport and support it with detailed analytical considerations. We use density functional theory (DFT) and density functional perturbation theory (DFPT) to compute vibrational modes and anharmonic coupling terms and calculate the scattering rates using perturbation theory. We have recently demonstrated that this approach gives excellent results for the linewidths and lineshifts of the optical phonon modes in graphene and graphite[16] as well as for the thermal transport properties of silicon−germanium alloys[17] and superlattices.[18]

To the lowest order in perturbation theory, the scattering rate (inverse lifetime) of a phonon mode $j$ at $\mathbf{q}$ is given by (see, e.g., ref 19):

$$\Gamma_j(\mathbf{q}) = \frac{\pi\hbar}{16N_{\mathbf{q}'}} \sum_{\mathbf{q}',j',j''} |V_3(j, -\mathbf{q}; j', \mathbf{q}'; j'', \mathbf{q}'')|^2 \times[(1 + n_{j'\mathbf{q}'} + n_{j''\mathbf{q}''})\delta(\omega_{j'\mathbf{q}'} + \omega_{j''\mathbf{q}''} - \omega_{j,\mathbf{q}}) + 2(n_{j''\mathbf{q}''} - n_{j'\mathbf{q}'})\delta(\omega_{j'\mathbf{q}'} - \omega_{j''\mathbf{q}''} - \omega_{j,\mathbf{q}})] \quad (1)$$

where $N_{\mathbf{q}'}$ is the number of $\mathbf{q}'$ points in the Brillouin zone (BZ), $n$'s are the Bose−Einstein phonon populations, $\omega$'s are taken as the harmonic phonon frequencies, $\mathbf{q}'' = -\mathbf{q} - \mathbf{q}' + \mathbf{G}$ ($\mathbf{G}$ is vector of the reciprocal space) and

$$V_3(j, \mathbf{q}; j', \mathbf{q}'; j'', \mathbf{q}'') = \sum_{\substack{LMlmn \\ \lambda\mu\nu}} \Phi_{\nu\mu\lambda}(0n, Mm, Ll) e^{i\mathbf{q}'\mathbf{R}_M} e^{i\mathbf{q}''\mathbf{R}_L} \times \frac{v^j_{n\nu}(\mathbf{q}) v^{j'}_{m\mu}(\mathbf{q}') v^{j''}_{l\lambda}(\mathbf{q}'')}{\sqrt{M_c{}^3 \omega_j(\mathbf{q}) \omega_{j'}(\mathbf{q}') \omega_f(\mathbf{q}'')}} \quad (2)$$

where $\Phi_{\nu\mu\lambda}(Nn, Mm, Ll)$ are the third derivatives of the energy with respect to the displacement of atoms $l$ $(m, n)$ in the $L(M, N)$-th unit cell along the Cartesian axis $\lambda$ $(\mu, \nu)$, $\mathbf{R}_L$ $(\mathbf{R}_M)$ is the position of the $L^{\text{th}}$ $(M^{\text{th}})$ unit cell, and the $v$'s are the phonon eigenvectors of the different modes. Note that the quasiparticle lifetimes computed using eq 1 include both Normal and Umklapp three-phonon processes. All the ingredients needed to calculate phonon lifetimes are computed using DFT and DFPT[20] as implemented in the Quantum-ESPRESSO distribution.[21] The parameters of the calculation are the same as described in ref 16. The third derivatives are calculated on a 5 × 5 × 1 supercell (see Supporting Information), and Fourier interpolation is used to compute quantities on fine grids in reciprocal space.

In order to accurately estimate the scattering rates of the acoustic phonon modes in graphene and the effect of strain on these quantities, a proper description of the acoustic modes in the long-wavelength limit is essential. In graphene at the equilibrium configuration (in absence of external forces), the LA and TA modes have a linear dispersion, while, due to rotational symmetry, the transverse out-of-plane ZA mode has a quadratic dispersion. Because of numerical inaccuracies, ab initio interatomic force constants (IFC) do not satisfy exactly the acoustic sum rules (ASR) related to traslational and rotational invariance of the system, and this can have significant effects on the dispersion of the acoustic modes. To solve this problem we have enforced these rules (see Supporting Information) on the IFC, and the effect of isotropic (positive) strain on the frequency of the acoustic modes has been computed via the third-order interatomic force constants—on which we have imposed the ASR due to translational invariance. In particular, the dynamical matrix of graphene under isotropic strain $\varepsilon$ is computed via

$$D^{\varepsilon}_{n\nu,m\mu}(\mathbf{q}) = D^{0}_{n\nu,m\mu}(\mathbf{q}) + \varepsilon \sum_{\substack{Ll\lambda \\ M}} \Phi_{\nu\mu\lambda}(0n, Mm, Ll) r_{Ll\lambda} e^{i\mathbf{q}\mathbf{R}_M} \quad (3)$$

where $D^0(\mathbf{q})$ is the dynamical matrix at $\mathbf{q}$ of the unstrained system. The effect of strain on the scattering rates is computed using the phonon modes of the strained system and the anharmonic terms of the unstrained one. Indeed, test calculations with third derivatives computed on 3 × 3 × 1 supercells of strained graphene (up to 1% of strain) show that scattering rates are not significantly affected by the small change in the anharmonic terms due to strain.

In Figure 1a we present the scattering rates of the in-plane acoustic modes in graphene along the Γ−$K$ direction in the BZ (the results around Γ do not depend significantly on the direction considered). In the long wavelength limit the two

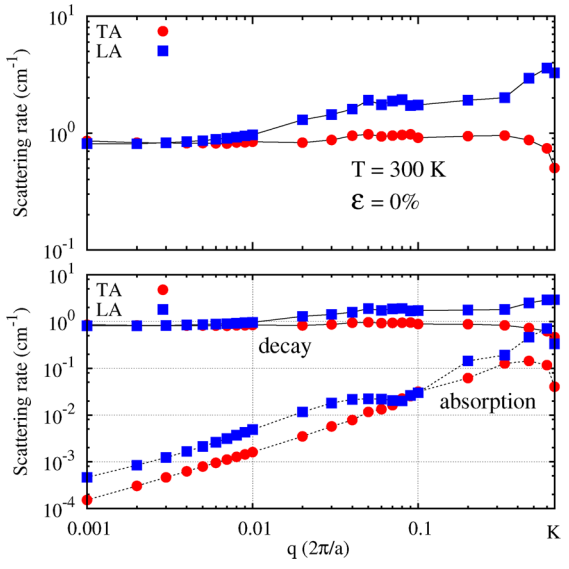


**Figure 1.** Upper panel: scattering rates for LA and TA modes along the Γ−$K$ direction in unstrained free-standing graphene at 300 K. Lower panel: Contributions to the scattering rates due to decay (solid lines) and absorption (dashed line) processes.


dx.doi.org/10.1021/nl202694m | Nano Lett. 2012, 12, 2673−2678

modes show a rate that tends to be a constant value of the order of 1 $cm^{-1}$ that corresponds to a lifetime of around 5 ps. As shown in Figure 1b the mechanism that determines this behavior is the decay of these modes into lower energy phonon branches. Note that in the long wavelength limit the contribution due to absorption processes is instead negligible as it tends to zero linearly with $q$. The analysis of the decay channels shows that the LA (TA) modes decay exclusively into two lower energy ZA modes through three-phonon Normal processes LA (TA) → ZA + ZA, and the existence of a finite scattering rate as $q \to 0$ is a direct consequence of the quadratic phonon dispersion of the ZA mode. To confirm analytically our numerical findings, we transform the 2D integral in eq 1 in a line integral:

$$\Gamma_j(\mathbf{q}) \propto \int_{C(\mathbf{q})} ds \frac{|V_3|^2(1 + n' + n'')}{|\nabla(\omega' + \omega'' - \omega)|} \quad (4)$$

where $C(\mathbf{q})$ is the locus of points defined by energy and momentum conservation. It is possible to show that because of the quadratic dispersion of the ZA mode, in the long wavelength limit $C(q)$ is a closed loop around Γ whose radius tends to $\mathbf{q} = 0$ as $\sqrt{q}$. As a consequence of this, in eq 4 $|V_3|^2$ goes as $q$ (see Appendix Section), and it cancels out the term containing the phonon population $n$'s (of the order $q^{-1}$); the gradient of the frequencies at the denominator goes as $\sqrt{q}$, and the integration on $ds$ ($\propto\sqrt{q}$) results in a constant scattering rate. This anomalous behavior is quite problematic from a fundamental point of view because it seems to imply that for very small wave vectors, the condition for the existence of phonons as elementary excitations $[\omega(\mathbf{q})\tau(\mathbf{q}) > 1]$ is not satisfied. Using our results, for LA (TA) mode, this would happen already for wavelength $\lambda > 0.9$ μm ($\lambda > 0.5$ μm), smaller than the typical size of samples used for thermal conductivity measurements.

It is interesting to observe that a similar behavior has been recently observed also in quasi 1D systems, such as nanotubes and linear chain of atoms.[22,23] In particular, Lindsay et al.[23] report a scattering rate for the longitudinal acoustic modes in nanotubes that diverges as $q \to 0$; as in graphene, this behavior is due to decay processes involving two bending modes with quadratic dispersion. Santhosh and Kumar[22] find a constant relaxation rate for the longitudinal modes of a linear atomic chain when the bare quadratic dispersion of the transverse mode is used in the calculation. To avoid the problem of not well-defined phonons, the authors use a self-consistent procedure to take into account the effects of anharmonicity on phonon dispersions. According to the authors, this procedure renormalizes the dispersion of the transverse mode, making it linear around $q = 0$, and allows to recover well-defined phonon modes. For graphene, and using renormalization group on a continuum model, Mariani and von Oppen[24] find that phonon−phonon interactions can renormalize the phonon frequency of the ZA mode, making it proportional to $q^{3/2}$ at small $q$.

A theoretical approach that goes beyond eq 1 to include in a rigorous way phonon−phonon interactions and, possibly, electron−phonon interactions is beyond the scope of this paper. Most importantly, we find that strain has a dramatic effect on long-wavelength dispersions and that it restores, even in infinitesimal amounts, the proper asymptoic behavior of scattering rates, with phonons now always well-defined even in the long-wavelength LA/TA case, rendering a full resolution of the complexities of the unstrained case less relevant—not to mention that even in practice strain will most likely be always present in finite amounts in suspended graphene.

In fact, the effect of strain on acoustic modes leads to qualitative changes in the phonon dispersions, as shown in Figure 2; while in-plane modes are only marginally affected by strain, the dispersion of the ZA modes varies dramatically, changing from quadratic to linear in the long wavelenght limit (with the linear term that, for small amount of strain, goes as $\sqrt{\varepsilon}$). This has strong effects on the scattering rates of the in-plane modes. Figure 3 shows that the contribution due to the decay into two ZA modes is not a constant, as in the case of unstrained graphene, but becomes proportional to $q^3$ and shows a $1/\varepsilon^3$ strain dependence at small $q$. The origin of the difference with respect to the unstrained case is that here,

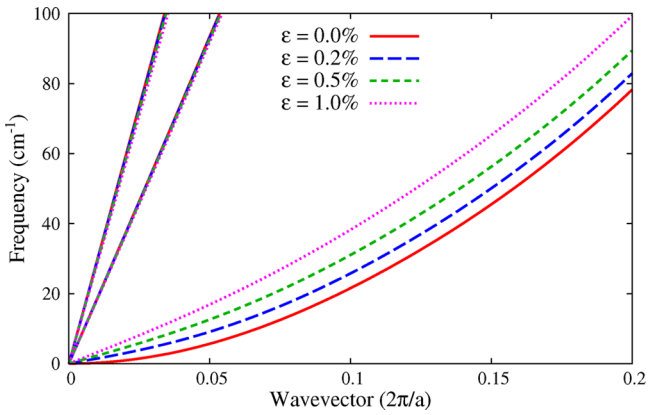


**Figure 2.** Dispersion of the acoustic phonon modes around Γ for different values of strain computed from eq 3. Around Γ the frequency of the ZA mode can be espressed as $\omega^2 = A(\varepsilon)q^2 + B(\varepsilon)q^4$, where $A(\varepsilon) = 1.01514 \times 10^7\varepsilon$ and $B(\varepsilon) = 5.22367 \times 10^6 - 1.6864 \times 10^7\varepsilon$ (the frequency is in $cm^{-1}$ and $\mathbf{q}$ is in $2\pi/a$, where $a$ is the lattice constant of graphene at the appropriate strain).

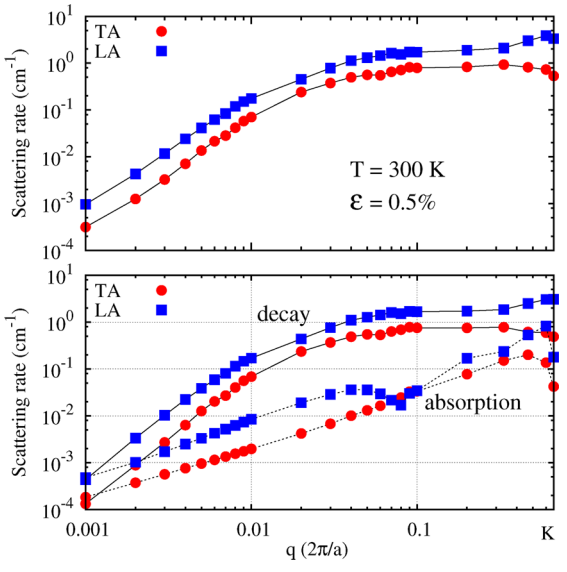


**Figure 3.** Same as in Figure 1 but for graphene under 0.5% isotropic strain. In the long wavelength limit the absorption contribution goes as $q$ and does not depend significantly on strain, while the decay contribution goes as $q^3$ and shows a $1/\varepsilon^3$ strain dependence.


dx.doi.org/10.1021/nl202694m | Nano Lett. 2012, 12, 2673−2678

because of the linear dispersion for the ZA mode, the radius of $C(\mathbf{q})$ tends to $q = 0$ linearly as $\mathbf{q} \to 0$. So, in eq 4, $|V_3|^2$ goes as $q^3$, the term $(1 + n' + n'')$ is of the order $q^{-1}$, while the gradient of the frequencies tends to a constant value. From Figure 3b one can see that in the long wavelength limit the total scattering rates are determined by the absorption processes, their contribution being linear in $q$ and almost unchanged with respect to the unstrained case [see Figure 1b]. The analysis of the absorption channels shows that the TA (LA) + LA → LA processes become the dominant ones.[25] The linearity of the relaxation rate can be understood considering eq 4 with $n'' - n'$ in place of $1 + n' + n''$ and $\omega' - \omega'' - \omega$ in place of $\omega' + \omega'' - \omega$. In this case the radius of $C(\mathbf{q})$ does not tend to $\mathbf{q} = 0$ as $q \to 0$, and it is easy to show that the term $n'' - n'$ is of order $q$, as is the gradient of the frequencies (since the two phonons involved in the absorption process belong to the same branch) and $|V_3|^2$ goes as $q$ (the Fourier tranform of the third-order IFC goes as $q$; the zero-order term being zero because of the ASR).

We now focus our attention on the out-of-plane acoustic modes. In the long wavelength limit the scattering rate for the ZA mode in unstrained graphene (Figure 4) goes as $q^2$, and this

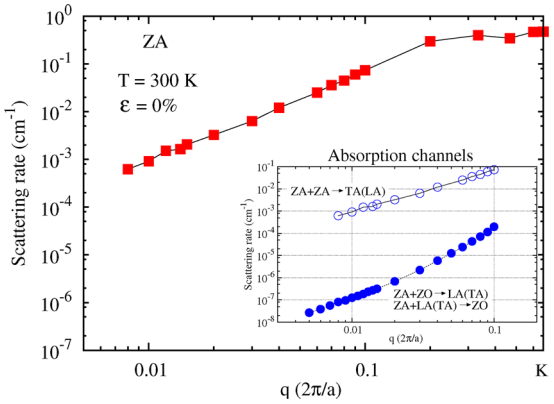


**Figure 4.** Scattering rates for the ZA phonon modes along the Γ−$K$ direction in unstrained graphene at 300 K. Inset: Contributions to the total rates: ZA + ZA → TA (LA) (open circles) and ZA + ZO → LA (TA) or ZA + LA (TA) → ZO (solid circles).

behavior is mainly due to ZA +ZA → LA(TA) absorption processes (it is possible to derive analytically this result along the lines of the case TA(LA) → ZA + ZA decay). There are other possible absorption channels—the main ones being ZA + ZO → LA (TA) or ZA + LA(TA) → ZO—that involve phonon modes near the crossing between the LA(TA) branches and the ZO branch. Their contribution at room temperature is smaller than the ZA + ZA → LA(TA) process but of the same order $q^2$. Also in this case the scenario changes when we apply strain (Figure 5). Because of the linear phonon dispersion of the ZA modes, the scattering rates due to ZA + ZA → LA(TA) are now proportional to $q^3$ (instead of $q^2$ as in the unstrained case) and show a $1/\sqrt{\varepsilon}$ strain dependence at small $q$. The contribution of the processes involving the ZO modes instead remains similar to the unstrained case (order $q^2$), and this makes these channels the dominant ones in the long wavelength limit ($q \to 0$). In passing, it is interesting to observe that the three-phonon relaxation processes of the ZA modes discussed here may provide a useful insight into the intrinsic dissipation mechanisms in graphene-based nano-electromechanical resonators.[26]

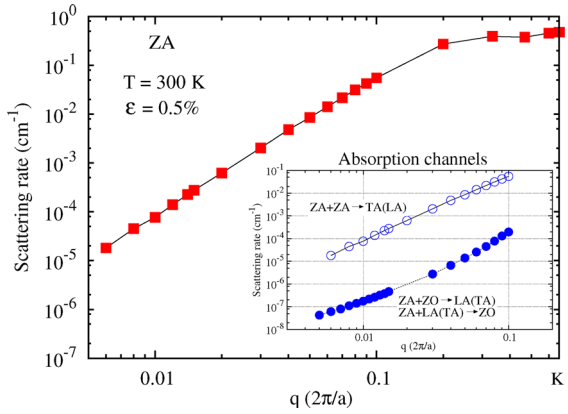


**Figure 5.** Same as in Figure 4 but for graphene under 0.5% isotropic strain. In the long wavelength limit the scattering rates due to decay processes involving ZO modes (solid squares) go as $q^2$ and are almost independent of strain, while the ZA + ZA → TA (LA) contributions (open circles) go as $q^3$ and show a $1/\sqrt{\varepsilon}$ strain dependence.

The results presented so far have fundamental consequences on the thermal transport properties of graphene. In submicrometer-sized unstrained graphene samples (but still large enough to be in the diffusive regime dominated by phonon−phonon interactions, see Supporting Information), standard perturbation theory results in well-defined phonon modes, and it is possible to extract information about the thermal conductivity $\boldsymbol{\sigma}$, using the single-mode relaxation time approximation (SMRTA) that gives $\boldsymbol{\sigma}$ in terms of frequencies, group velocities, and lifetimes $\tau = 1/\Gamma$ (calculated under the assumption that all the other modes are in thermal equilibrium and including only three-phonon processes): $\sigma \propto \int dq^2 v^2 \omega^2 n(n + 1)\tau$. We find a value for $\boldsymbol{\sigma}$ of around 550 W/(mK) at room temperature that is dominated by the ZA modes carrying around 50% of the heat. We expect this to be a lower limit for $\sigma$ since the SMRTA usually underestimates the solution of Boltzmann transport equation. In particular, it is important to point out that in the case of graphene the SMRTA may lead to a quite substantial underestimation of the actual thermal conductivity because the long wavelength behavior of the acoustic modes is dominated by Normal processes and their resistive contribution may be significantly overestimated within SMRTA (where Normal and Umklapp processes contribute on an equal footing). For larger samples, standard perturbation theory is not adequate to explain thermal transport in graphene, and more sophisticated methods and further work are necessary to recover well-defined elementary excitations in the long-wavelength limit and to elucidate their role in thermal transport.

In the case of strained graphene, phonons are instead always well-defined ($\omega\tau \gg 1$ at room temperature), and thermal transport is dominated by ZA flexural modes. Indeed, while the contribution to $\sigma$ of the LA and TA modes is finite (and in particular does not depend on system size), the contribution of the flexural modes diverges logarithmically with the size of graphene samples. It is important to stress that the divergence of $\sigma$ is not an artifact of the SMRTA (given that it underestimates conductivity), even if higher-order phonon processes or extrinsic phonon scattering mechanisms could modify this picture. In particular, boundary scattering can strongly attenuate the magnitude of the expected divergence (see Supporting Information). In passing it is also noteworthy to observe that since room temperature thermal conductivity in


dx.doi.org/10.1021/nl202694m | Nano Lett. 2012, 12, 2673−2678

graphene is crucially dependent upon acoustic modes, whose energy is much smaller than kT, and thus with the Bose–Einstein distribution almost indistinguishable from the Maxwell–Boltzmann one, classical simulations (e.g., molecular dynamics) should also be able to capture correctly the key features of heat transport.

Last, we point out that the quasiparticle relaxation times discussed here are measurable quantities. This means that the results of this paper, including intrinsic stability and lifetimes of the acoustic phonons and the role of strain and systems size, can be directly accessed in experiments. This is particularly true when one considers the energy resolution of current experimental techniques that can effectively probe acoustic phonon lifetime effects. For instance, the energy resolution in neutron spin–echo spectroscopy is about $10^{-6}$ eV (~0.008 $cm^{-1}$) (see, for instance, ref 27), and helium spin–echo spectroscopy used in surface science can be even more sensitive (see, for instance, ref 28). Given the large experimental uncertainty in the estimation of the thermal conductivity, it seems crucial to exploit such complementary tools to accurately characterize the dynamics of acoustic phonons that determine the thermal properties of graphene.

In summary, we have calculated fully from first-principles the lifetimes of long-wavelength acoustic phonons in graphene and discussed their role in determining the thermal conductivity of this material. The calculations have also been supported by detailed analytical models. In free-standing graphene, the lifetimes of TA and LA phonons converge to a finite value in the long-wavelength limit, making long-wavelength phonons as calculated by standard perturbation theory too short-lived to transverse their own wavelength. Mechanical strain linearizes the quadratic dispersion of the ZA modes around $\mathbf{q} = 0$, removing decay channels for the long-wavelength LA and TA phonons and restoring the correct asymptotic behavior for their lifetimes. Remarkably, the thermal conductivity is predicted to diverge with system size for any amount of applied strain, due to the contributions of the long-wavelength flexural ZA modes. On the other hand, extrinsic factors, such as boundary scattering, can significantly renormalize such effect. These findings indicate that built-in strain, sample size, and device geometry are factors of paramount importance when trying to understand or engineer thermal transport in free-standing graphene and that acoustic phonon lifetimes could represent a very sensitive albeit challenging probe of the experimental conditions.

Finally, we note that since thermal transport in graphene is determined by the anomalous dispersion of the acoustic phonons, the microscopic analysis presented here can be of particular interest also in other materials that present similar dispersions, including other low-dimensional systems as well as materials near lattice instabilities and mode softening.

## APPENDIX

### Analytic Limit of the Scattering Rates

In the long wavelength limit the lifetime of the in-plane acoustic modes of unstrained graphene tends to a constant value; this behaviour is due to the decay processes that involve two ZA modes. Here we present a derivation of the analytic limit of the contribution of these processes to $\tau$. The inverse lifetime is given by

$$\frac{1}{\tau_i(\mathbf{q}_i)} \propto \sum_{\mathbf{q}_f} |V_3(\mathbf{q}_i, \mathbf{q}_f)|^2 \{n[\omega_f(\mathbf{q}_f)] + n[\omega_f(\mathbf{q}_i + \mathbf{q}_f)] + 1\} \times \delta[\omega_i(\mathbf{q}_i) - \omega_f(\mathbf{q}_f) - \omega_f(\mathbf{q}_i + \mathbf{q}_f)] \quad (5)$$

where

$$V_3(\mathbf{q}_i, \mathbf{q}_f) = \sum_{\substack{LMlmn \\ \lambda\mu\nu}} \Phi_{\nu\mu\lambda}(0n, Mm, Ll) e^{i\mathbf{q}_f \mathbf{R}_M} e^{-i(\mathbf{q}_i+\mathbf{q}_f)\mathbf{R}_L} \times \frac{v^i_{n\nu}(\mathbf{q}_i) v^f_{m\mu}(\mathbf{q}_f) v^f_{l\lambda}(-\mathbf{q}_i - \mathbf{q}_f)}{\sqrt{M_c{}^3 \omega_i(\mathbf{q}_i)\omega_f(\mathbf{q}_f)\omega_f(\mathbf{q}_i + \mathbf{q}_f)}} \quad (6)$$

Here the index $i$ is for the initial LA (TA) phonon mode and the index $f$ is for the final ZA modes. In the limit of very small wavevectors we can assume $\omega_i(\mathbf{q}) = Aq$, $\omega_f(\mathbf{q}) = Bq^2$ (where $q = |\mathbf{q}|$) and the following form for the eigenvectors:

$$v^{\mathrm{LA}}_{l\lambda}(\mathbf{q}) = \frac{1}{\sqrt{2}} \frac{q_\lambda}{q} e^{i\mathbf{q}\mathbf{r}_l}$$

$$v^{\mathrm{TA}}_{l\lambda}(\mathbf{q}) = \frac{1}{\sqrt{2}} \frac{q^\perp_\lambda}{q} e^{i\mathbf{q}\mathbf{r}_l}$$

$$v^{\mathrm{ZA}}_{l\lambda}(\mathbf{q}) = \frac{1}{\sqrt{2}} \delta_{z\lambda} e^{i\mathbf{q}\mathbf{r}_l} \quad (7)$$

where $\mathbf{r}_l$ is the position of atom $l$ in the unit cell and $\mathbf{q}^\perp$ is the vector $(q_y, -q_x)$. Using polar coordinates, we set $\mathbf{q}_i = (q_i, 0)$ (without loss of generality) and $\mathbf{q}_f = q_f(\cos\theta, \sin\theta)$. Energy conservation requires $\Delta E = Aq_i - 2Bq_f^2 - Bq_i^2 - 2Bq_iq_f \cos\theta = 0$, and this defines a loop around $\mathbf{q}_i$. In the limit of $q_i \to 0$, $q_f^0$ (for which there energy is conserved) goes as $\sqrt{q_i}$. The integral in eq 5 can be rewritten in polar coordinates

$$\frac{1}{\tau_i(\mathbf{q}_i)} = \int_0^{2\pi} d\theta \int_0^\infty dq_f q_f F(q_i, q_f, \theta) \delta[\Delta E(q_i, q_f, \theta)] = \int_0^{2\pi} d\theta \left. \frac{q_f F(q_i, q_f, \theta)}{\left| \frac{\partial \Delta E(q_i, q_f, \theta)}{\partial q_f} \right|} \right|_{q_f = q_f^0} \quad (8)$$

where

$$F = |V_3|^2 \{n[\omega_f(\mathbf{q}_f)] + n[\omega_f(\mathbf{q}_i + \mathbf{q}_f)] + 1\} \quad (9)$$

In eq 8 the derivative of $\Delta E$ goes as $\sqrt{q_i}$ for $q_i \to 0$ and cancels exactly $q_f$ at the numerator. In the following we show that the function $F$ instead tends to a constant. The term $n[\omega_f(\mathbf{q}_f)] + n[\omega_f(\mathbf{q}_i + \mathbf{q}_f)] + 1$ goes as $q_i^{-1}$ for $q_i \to 0$. For the LA mode polarized in the $x$ direction, for example, eq 6 becomes

$$V_3(\mathbf{q}_i, \mathbf{q}_f) \propto \sum_{LMlmn} \Phi_{xzz}(0n, Mm, Ll) \times \frac{e^{i\mathbf{q}_i(\mathbf{r}_n - \mathbf{r}_{Ll})} e^{i\mathbf{q}_f(\mathbf{r}_{Mm} - \mathbf{r}_{Ll})}}{\sqrt{q_i q_f^2 |\mathbf{q}_i + \mathbf{q}_f|^2}} \quad (10)$$

The denominator of this expression goes as $q_i^{3/2}$ for $q_i \to 0$. In order to find the behavior of the numerator we need to expand the exponential in powers of $q_i$. We find that the lowest order terms ($1$, $q_i^{1/2}$, $q_i$, and $q_i^{3/2}$) are zero and the first non-zero term is quadratic in $q_i$. In particular: (1) The term that does not depend on $q_i$ is zero because of the acoustic sum rule due to the translational invariance of the system:


dx.doi.org/10.1021/nl202694m | Nano Lett. 2012, 12, 2673–2678

$$\sum_{Ll} \Phi_{\nu\mu\lambda}(0n, Mm, Ll) = 0$$

and analogous rules obtained by permutation of the indexes; (2) The term in $q_i^{1/2}$ contains the sum

$$\sum_{LMlm} \Phi_{xzz}(0n, Mm, Ll)[\mathbf{q}_f \cdot (\mathbf{r}_{Mm} - \mathbf{r}_{Ll})] \tag{11}$$

that is zero because the terms in the sum change sign when exchanging $\{Mn\}$ with $\{Ll\}$; (3) The contribution in $q_i$ is

$$\sum_{LMlmn} \Phi_{xzz}(0n, Mm, Ll)\{i\mathbf{q}_i \cdot (\mathbf{r}_n - \mathbf{r}_{Ll}) - [\mathbf{q}_f \cdot (\mathbf{r}_{Mm} - \mathbf{r}_{Ll})]^2\} \tag{12}$$

The term in $\mathbf{q}_i$ is zero because of the translational acoustic sum rule. The term in $q_f$ vanishes because of a cancellation of terms

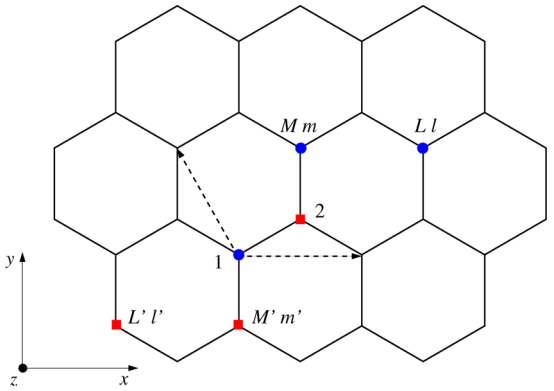


**Figure 6.** Cancellation of terms in eqs 12 and 13. Because of symmetry $\Phi_{xzz}(01, Mm, Ll) = -\Phi_{xzz}(02, M'm', L'l')$. In eq 12 $[\mathbf{q}_f \cdot (\mathbf{r}_{Mm} - \mathbf{r}_{Ll})]^2 = [\mathbf{q}_f \cdot (\mathbf{r}_{M'm'} - \mathbf{r}_{L'l'})]^2$ and in eq 13 $[\mathbf{q}_i \cdot (\mathbf{r}_2 - \mathbf{r}_{Ll})][\mathbf{q}_f \cdot (\mathbf{r}_{Mm} - \mathbf{r}_{Ll})] = [\mathbf{q}_i \cdot (\mathbf{r}_1 - \mathbf{r}_{L'l'})][\mathbf{q}_f \cdot (\mathbf{r}_{M'm'} - \mathbf{r}_{L'l'})]$. In the sums over $n$, $Mm$, $Ll$ in eqs 12 and 13, the contributions coming from the red (squares) and the blue (circles) groups of atoms cancel exactly. Dashed lines represent graphene lattice vectors.

as schematically explained in Figure 6; and (4) The term in $q_i^{3/2}$ contains

$$\sum_{LMlmn} \Phi_{xzz}(0n, Mm, Ll)\{[i\mathbf{q}_f \cdot (\mathbf{r}_{Mm} - \mathbf{r}_{Ll})]^3 - [\mathbf{q}_i \cdot (\mathbf{r}_n - \mathbf{r}_{Ll})] [\mathbf{q}_f \cdot (\mathbf{r}_{Mm} - \mathbf{r}_{Ll})]\} \tag{13}$$

Here the term in $[i\mathbf{q}_f \cdot (\mathbf{r}_{Mm} - \mathbf{r}_{Ll})]^3$ vanishes similarly to eq 11. The second term vanishes as explained in Figure 6.

In a similar way it is possible to determine the analytic limit of the lifetime of the acoustic modes when the dispersion of the ZA is not quadratic.

## ■ ASSOCIATED CONTENT

### Supporting Information

Supporting Information about the accuracy of the third-order force constants and the dispersion of the ZA mode are available. This material is available free of charge via the Internet at http://pubs.acs.org.

## ■ AUTHOR INFORMATION

### Corresponding Author

*E-mail: nicola.bonini@kcl.ac.uk

### Notes

The authors declare no competing financial interest.

## ■ ACKNOWLEDGMENTS

J.G. acknowledges support from MIT Institute for Soldier Nanotechnologies (ISN-ARO).

## ■ REFERENCES

(1) Balandin, A. A.; et al. *Nano Lett.* **2008**, *8*, 902.
(2) Ghosh, S.; et al. *Appl. Phys. Lett.* **2008**, *92*, 151911.
(3) Balandin, A. A. *Nat. Mater.* **2011**, *10*, 569.
(4) Faugeras, C.; Faugeras, B.; Orlita, M.; Potemski, M.; Nair, R. R.; Geim, A. K. *ACS Nano* **2010**, *4*, 1889.
(5) Cai, W.; Moore, A. L.; Zhu, Y.; Li, X.; Chen, S.; Shi, L.; Ruoff, R. S. *Nano Lett.* **2010**, *10*, 1645.
(6) Chen, S.; Moore, A. L.; Cai, W.; Suk, J. W.; An, J.; Mishra, C.; Amos, C.; Magnusson, C. V.; Kang, J.; Shi, L.; Ruoff, R. S. *ACS Nano* **2011**, *5*, 321.
(7) Seol, J. H.; Jo, I.; Moore, A. L.; Lindsay, L.; Aitken, Z. H.; Pettes, M. T.; Li, X.; Yao, Z.; Huang, R.; Broido, D.; Mingo, N.; Ruoff, R. S.; Shi, L. *Science* **2010**, *328*, 213.
(8) Lee, J.-U.; Yoon, D.; Kim, H.; Lee, S. W.; Cheong, H. *Phys. Rev. B* **2011**, *83*, 081419(R).
(9) Lepri, S.; Levi, R.; Politi, A. *Phys. Rep.* **2003**, *377*, 1.
(10) Donadio, D.; Galli, G. *Phys. Rev. Lett.* **2007**, *99*, 255502.
(11) Klemens, P. G. Int. *J. Thermophys.* **2001**, *22*, 265.
(12) Klemens, P. G.; Pedraza, D. F. *Carbon* **1994**, *32*, 735.
(13) Mounet, N.; Marzari, N. *Phys. Rev. B* **2005**, *71*, 205214.
(14) Mingo, N.; Broido, D. A. *Phys. Rev. Lett.* **2005**, *95*, 096105.
(15) Lindsay, L.; Broido, D. A.; Mingo, N. *Phys. Rev. B* **2010**, *82*, 115427.
(16) Bonini, N.; Lazzeri, M.; Marzari, N.; Mauri, F. *Phys. Rev. Lett.* **2007**, *99*, 176802.
(17) Garg, J.; Bonini, N.; Kozinsky, B.; Marzari, N. *Phys. Rev. Lett.* **2011**, *106*, 045901.
(18) Garg, J.; Bonini, N.; Marzari, N. *Nano Lett.* **2011**, *11*, 5135.
(19) Srivastava, G. P. *The physics of phonons*; Taylor & Francis Group: New York, 1990.
(20) Baroni, S.; de Gironcoli, S.; Dal Corso, A.; Giannozzi, P. *Rev. Mod. Phys.* **2001**, *73*, 515.
(21) Giannozzi, P.; et al. *J. Phys.: Condens. Matter* **2009**, *21*, 395502.
(22) Santhosh, G.; Kumar, D. *Phys. Rev. E* **2010**, *82*, 011130.
(23) Lindsay, L.; Broido, D. A.; Mingo, N. *Phys. Rev. B* **2009**, *80*, 125407.
(24) Mariani, E.; von Oppen, F. *Phys. Rev. Lett.* **2008**, *100*, 076801.
(25) The absorption process LA + LA → LA that determines the long wavelength behavior of the scattering rate of the LA mode seems to be quite delicate and probably sensitive to small variations of the shape of the dispersion of the LA mode. Indeed, considering the absorption channels of a LA mode at a $q_0$ close to Γ the function $\Delta E(\mathbf{q}) = \omega_{LA}(\mathbf{q}_0) + \omega_{LA}(\mathbf{q}) - \omega_{LA}(\mathbf{q} + \mathbf{q}_0)$ has a small locus of points corresponding to $\Delta E(\mathbf{q}) = 0$ but also shows a negative minimum very close to zero.
(26) Chen, C.; et al. *Nat. Nanotechnol.* **2009**, *4*, 861.
(27) Keller, T.; Aynajian, P.; Habicht, K.; Boeri, L.; Bose, S. K.; Keimer, B. *Phys. Rev. Lett.* **2006**, *96*, 225501.
(28) Alexandrowicz, G.; Jardine, A. P. *J. Phys.: Condens. Matter* **2007**, *19*, 305001.